Visual Abstract

J integral computation and limit load analysis of bonded composite repair in cracked pipes under pressure

M. Belhamiani, D. E. Belhadri, W. Oudad, O. Mansouri, W. N. Bouzitouna
Smart Structures Laboratory Univ Ctr of Ain Témouchent, Po Box 284,46000, Algeria
mbelhamiani@gmail.com, https://orcid.org/0000-0001-8951-032X
djamelins@hotmail.fr
oudadw@gmail.com, https://orcid.org/0000-0002-3283-1322
omansouri81@gmail.com
hibanesrine@outlook.fr

ABSTRACT. In this paper an additional criterion was introduced to evaluate the composite repair systems using the limit load analysis. The plastic collapse pressure of API 5L X65 PSL2 steel pressure vessel structure with crack defect is numerically investigated after the structure was been repaired by composite overwrap. The objective of this study was the analysis of the efficiency of composite repair systems using this additional criterion to gain more confidence on it taking into account, the cracks and the overwrap geometries. The material of the pipe is elastic perfectly plastic for the plastic collapse pressure criterion and elastic-plastic using the Romberg Osgood model for fracture mechanic criterion. The additional criterion allows us to compare the uncracked and cracked pipe to estimate the repair efficiency. Moreover, the composite overwrap could restore 90% of the plastic collapse pressure for cracked pipes.

KEYWORDS. J integral; API 5L X65; Limit load; Romberg Osgood model; crack; Pipe.

OPEN ACCESS

Citation: Belhamiani, M., Belhadri, D. E., Oudad, W., Mansouri, O., Bouzitouna, W., N., J integral computation and limit load analysis of bonded composite repair in cracked pipes under pressure, Frattura ed Integrità Strutturale, 50 (2019) 623-637.

Received: 09.08.2019
Accepted: 10.09.2019
Published: 01.10.2019

INTRODUCTION

Traditionally, mechanical defects in pipes and pipelines which have been detected either by working on the pipeline or by intelligent pigging have been repaired by replacing the defective areas. The use of thermosetting plastics and reinforcing fibers has a long and varied history of being used as a repair material for structural repairs. The fabric options consist primarily of Carbon, Kevlar or Glass fibers, which are bound together and bonded to the pipe with various resin options [1].

The problematic in this work lies in the difficulty of i) finding a global criterion for comparing the state of a cracked pipe to the reference state means uncracked pipe in the first place and a pipe repaired by this technique to the same reference state. ii) The difficulty is how to define precisely the field of the application of stress intensity factor SIF (K_1) and J integral criterion. iii) Also, there is a difficulty to specify a referential of the crack front to be studied. iv) The SINTAP procedure cannot estimate the safety status of an uncracked pipe's find a criterion which can quantify the state of security of a pipe in the presence of several defects at the same time such as a crack, a thermic affected zone, a welding and a loss of material. To deal with this problems, in this work we have chosen to use an additional criterion which is the plastic collapse pressure, this approach raises an important operational problem: by quantifying the state of the structure by a measurable parameter is more efficient and even more exact than to express it by a computable parameter (SIF and integral *J*) and which strongly depends on the referential point. Moreover, in technical terms: in industry it is better to value the repair by a parameter that can easily be understood and managed as the limit pressure rather than a computable parameter.
There are eight potential modes or mechanisms of failure that must be avoided according to the ASME code criterion between these modes, the excessive plastic deformation under a static load. The ASME Section VIII Div 2 5.2 (ASME Designe by analyses DBA) [2] define the procedure for assessment of plastic collapse based on elastic-plastic analysis methods. In this study, the procedures for limit and elastic-plastic design are considered.

EVALUATION CRITERIA

First criterion: The J integral

In the theory of linear elasticity, a crack introduces a discontinuity in the structure where the stresses tend to infinity in the vicinity of the crack tip. Using the semi-inverse method of Westergaard [3], Irwin [4, 5] related the singular behavior of the stress components to the distance to the crack tip. Based on the deformation theory of plasticity, Rice [6] proposed a new fracture parameter to predict the crack growth, based on path-independent contours that was called J integral and defined as:

$$J = \oint_C (wdy - T_i \frac{\partial u_i}{\partial x} ds) \tag{1}$$

where C is an arbitrary curve around the tip of a crack, w is the strain energy density, T_i is the components of the traction vector, u_i is the displacement vector components, ds is the length increment along the contour, x and y are the rectangular coordinates with the y direction taken normal to the crack line and the origin at the crack tip.
Kobayashi et al. [7] verified this path independence by the finite element analysis (FEA)For power-law hardening materials, Hutchinson [8] and Rice and Rosengren [9] evaluated independently the character of crack-tip stress fields. Researchers Rice and Rosengren have studied the conditions of plane deformation while Hutchinson studied both the conditions of stress and deformation planes. Rice and Rosengren obtained essentially identical results to Hutchinson's solutions in a different format. For a power-law hardening material, as pointed out by McClintock [10], Hutchinson obtained the following asymptotic solutions of crack-tip stress and strain fields:

$$\sigma_{ij} = \sigma_0 \left(\frac{J}{\sigma_0 \varepsilon_0 I_n r} \right)^{\frac{1}{n+1}} \widetilde{\sigma}_{ij}(n,\theta) \tag{2}$$

$$\varepsilon_{ij} = \alpha \varepsilon_0 \left(\frac{J}{\sigma_0 \varepsilon_0 I_n r} \right)^{\frac{n}{n+1}} \widetilde{\varepsilon}_{ij}(n,\theta) \tag{3}$$

where $\varepsilon_0 = \sigma_0/E$, σ_0 is a reference stress, n is the strain hardening exponent, I_n is an integration constant that depends on n, σ_{ij} and ε_{ij} are the dimensionless functions of n and h.
This solution is called the HRR field. The J-integral and HRR has laid a solid foundation for the EPFM theory.

Second criterion: The limit load analysis

The development of finite element methods and computational tools has stimulated limit stress analysis for complex structures. Koopman and Lance [11] analysed the plastic limit load using nonlinear mathematical programming firstly in 1965. after that they used this method to analyze the 2D plate and symmetry shell structure [12]. In 1989 Berak and Gerdeen [13] developed a P-norm method based on lower bound method of limit load, and then Liu et al in 1995. [14–15] analyzed the limit load for 3D structure, they used the penalty-duality algorithm and direct iteration method to analyze the pressure vessels with volume defects, taking into account the failure modes for different defects. Recently in 2002, Yun.J et al [16] quantified the effect of the crack shape, semi-elliptical or rectangular on the limit load pressure. Peng.F et al [17] proposed theoretical method to calculate a plastic collapse load for pressure vessel under internal pressure compared with ASME Boiler pressure vessel code.in 2015 X.-T. Mioa et al [18] analysed a limit loads for CT specimen based on the XFEM compared with EPRI method, twice slope method and J_{IC} criterion, they concluded that the XFEM is useful method to estimate the limit load for cracked structure.

GEOMETRICAL AND MATERIALS MODELS:

Fig. 1 illustrates the geometrical characteristics of the model. It should be noted that for the cracked pipe, R is the outer radius R_o= 177.8mm, L_P is the longitudinal length L_P= 1000 mm, and t=12.7 mm is the wall's thickness. The cracks were repaired by using a Glass-epoxy composite patch bonded cylinder form with an adhesive cylinder (FM 73). The width of the repair patches is ep_{comp}= 7mm and adhesive thickness is ep_{adh}= 0.2 mm the overwrap has 200mm of length (L), the interaction surfaces are supposed to be perfect between pipe / adhesive and adhesive / composite. The end sections pipeline was subjected to no displacement in z direction (u_3=0). The material properties of the pipeline, patch, and adhesive are summarized in Tab. 1. The pipe was made of X65 grade steel per API 5L X65 PSL2 [19] specifications. The stress–strain relationship was defined using the Ramberg–Osgood material model expression [20]:

$$\varepsilon(\sigma)=\frac{\sigma}{E}+\alpha\left(\frac{\sigma}{E}\right)^{n} \tag{4}$$

API 5L X65 properties [19]	
Young's modulus (GPa)	205
Poisson's ratio	0.3
Minimum yield stress (MPa)	415
Yield strain	0.5%
Ramberg–Osgood's model yield offset (α)	1.48
Strain hardening component (n)	18.99
Glass epoxy composite properties [21]	
Young's modulus E_1(GPa)	55
Young's modulus E_2 , E_3 (GPa)	15.2
Poisson's ratio ν_{12}, ν_{13}	0.254
Poisson's ratio ν_{23}	0.428
Shear modulus (GPa)	4.7
Adhesive FM73 properties [22]	
Young's modulus (GPa)	3.28
Poisson's ratio	0.45

Table 1: Material's properties.

The Ramberg–Osgood model was found to represent the relationship accurately, with its parameters extracted from Walker and Williams [21].

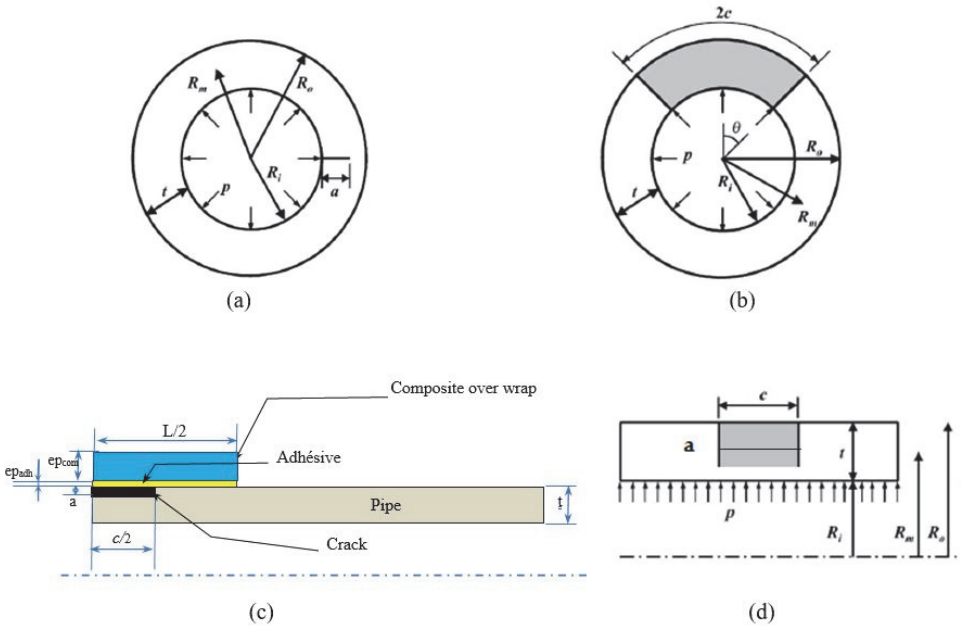

Figure 1: Geometries and dimensins considered in the present work [23]: (a) plane strain pipe with an extended inner axial crack, (b) circumferential through wall cracked pipe, (c) repaired pipe and (d) axial through wall cracked pipe.

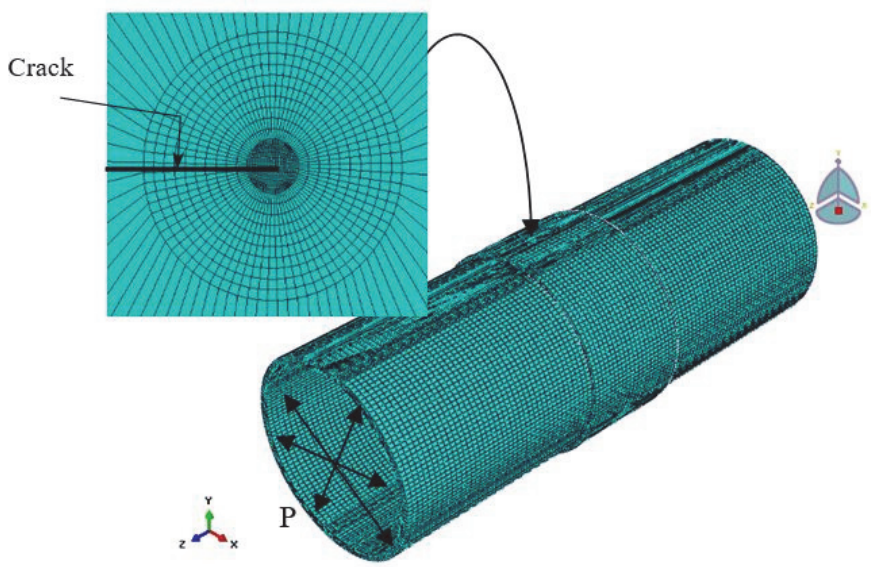

Figure 2: Mesh type of the model and reffined crack front for all crack type

FINITE ELEMENT MODEL

The FE code ABAQUS was used in this work to obtain the stress fields of the pipeline and the J integral versus the longitudinal crack front.

The FEM was used to model the cracked pipeline repaired by a wrap composite. The FE mesh for the longitudinal crack is shown in Fig. 2. The pipeline was meshed using a structured mesh with three-dimensional hex-dominated quadratic elements (C3D20R). In order to improve accurately the J integral values calculated from the crack geometry, the simulation on crack zone is performed using the 20-node brick elements with high-level mesh refinement

near the crack tip with an element dimension of 0.06mm [24]. Fig. 2 shows the mesh of the specimen and the mesh refinement in the crack tip region. The variation of diverse crack parameters by repairing the crack was investigated.
We used in the step option, the static general to analysis the first criterion and the static risks was applied to calculate the limit load.

RESULTS AND DISCUSSION

In what follows we will use the variables J* and PLP*, which will represent the improvement provided by the repair where:

$$J^{*} = \frac{J^{unrepaired} - J^{repaired}}{J^{unrepaired}} \tag{5}$$

$$PLP^{*} = \frac{PLP^{repaired} - PLP^{unrepaired}}{PLP^{unrepaired}} \tag{6}$$

First criterion

The pipeline was subjected to an applied internal pressure of P = 7 MPa, and the longitidinale crack geometrie was defined in Fig.1(d).

a. Choice of the reference point

The maximum of J inegral in crack tip line (1) and (2) by loading pressure as shown in Fig. 3.
Fig. 3 shows the *J* integral distribution along the crack tip line (1) for a longitudinal crack for a repaired pipe. As seen that the maximum values of J integral lie in the middle of the crack tip, which implies that the crack tends to propagate radially more than longitudinally. Also, this figure shows that at c/t=10 the maximum value of the J integral remains constant and independent of the crack length. As an example, for a c/t =10 to 15.75 the *J* =1.1 J/mm². in other words, the repaired system blocks the rise of the *J* integral by a good absorption of stresses when the ration c/t exceeds 10 and length recovery composite L=200mm.
To confirm the result, Fig. 4 presents the variation of maximum *J* integral value in the crack tip line (1,2) with the loading pressure for both repaired and unrepaired pipes.
In what follows we will consider the middle of the crack tip line (1) as a reference point for the entire study.

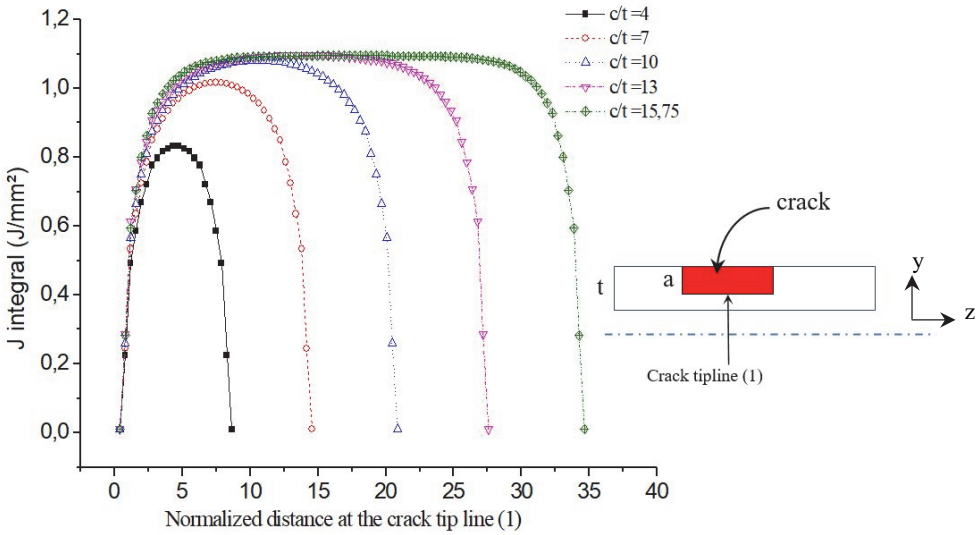

Figure 3: *J* integral distribution along the crack tip line (1) for longitudinale crack for repaired pipe(a/t=0.5)

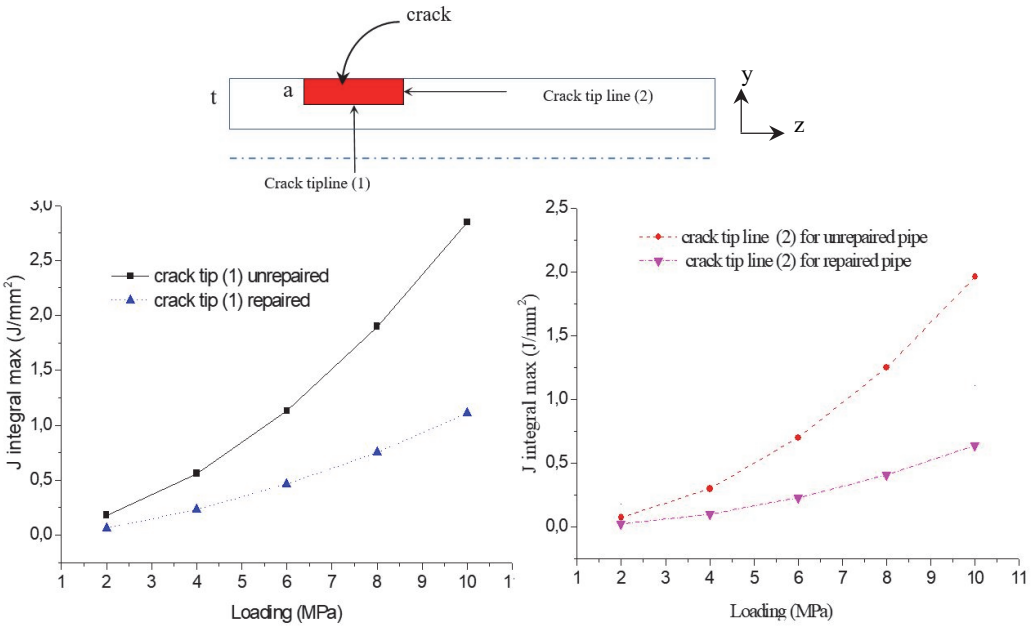

Figure 4: The variation of maximum J integral value in the Crack tip (1,2) with the loading pressure.

We outcome in the fig.4 a nonlinear prportionality behavior of the value of maximum of J integral with loading pressure, this latter is due to the elastic plastic behaviore of the API 5L X65 PSL2 pipe and the existence of an important plastic zone in the vicinity of the front of crack. In our case of study the J integral max of the line 1 and slightly higher of the line 2 for the unrepaired pipe and repaired respectively 33% and 50%. This is probably due to the non-symmetry of crack geometry and stress distribution in the crack boundary.
Also we can note that the crack propagation in depth is more dangerous than the longitudinal crack. This is for the repaired and unrepaired pipe.

b. Crack length

From the analysis of Fig.3 and to analyze the effect of the crack length one limits oneself in this study of the value c/t=2. In the Fig 5 some plots are shown which refer to the behaviore of J integral max (a) and the J* (b) vs crack length . It must be appointed that the J integral max increase as the crack length increase . This behaviour increases the risk of pipe rupture.

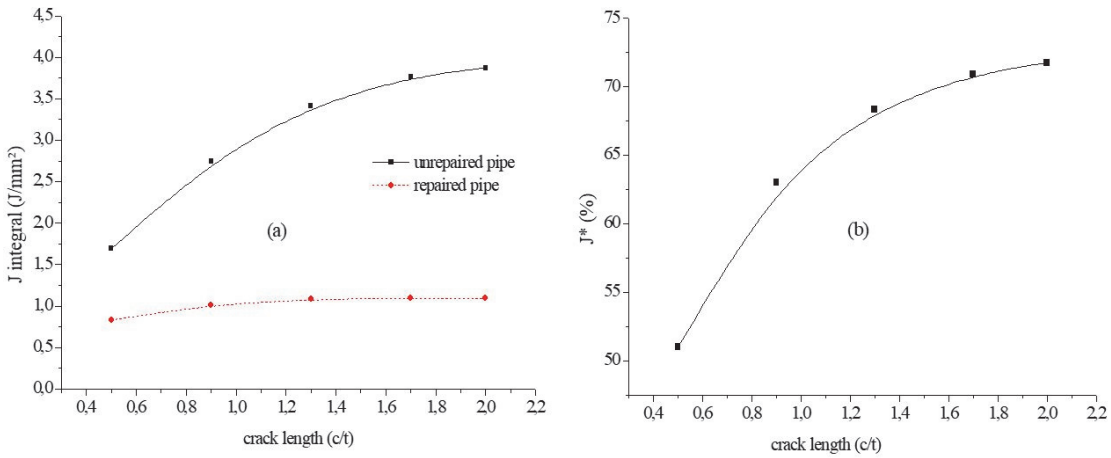

Figure 5: The variation of the J integral for repaired and unrepaired pipe and J* with the crack length (a/t=0.5).

The *J* integral max tends to stablize when c/t > 1 for repaired pipe and the composite overwrap reduces the *J* integral level for a constante value (1.1 J/mm²) beyond 85% of c/t fig .5a. In the other hand, the J* confirm this observation where J* remain independent to c/t for crack length greater than 1,8 of c/t. This can be explained by the level of reaction of the repair system which reaches 72% of its efficiency.

c. Patch length

In Fig. 6 the variation of the J integral and J* are presented in function of the patch length, As seen in Fig.6 the J*increases rapidly to reach a upper limit with a patch length of the order of 15.75(L / t) with 51% of its maximum efficiency, than the efficiency of the repair system begins to decrease after 15.75 (L/t). This is due to the moment created in the end section of the patch which favours the opening of the crack, This remark has also been signaled by Ahmed Shouman et *al* [25].

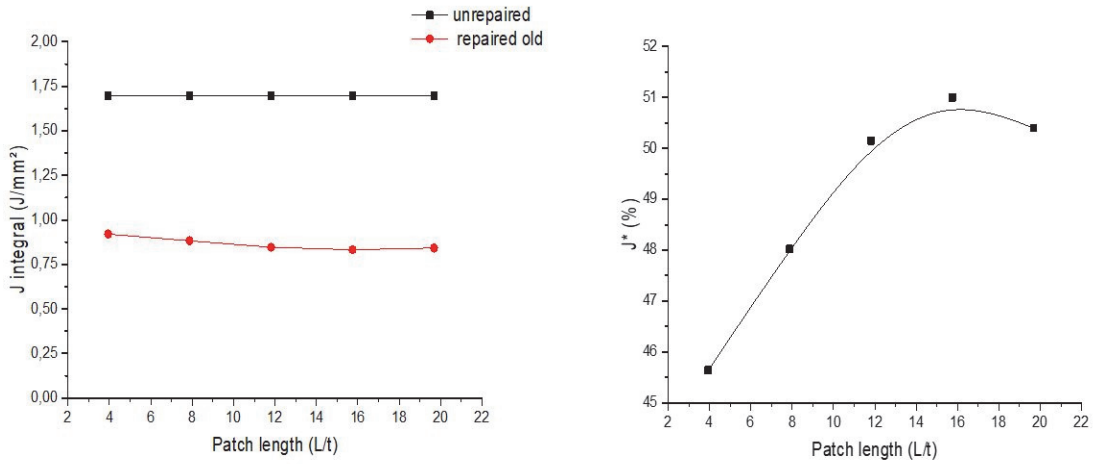

Figure 6: The variation of the J integral and J* with the patch length for repaired and unrepaired pipe. (a/t=0.5)

It can be concluded that increasing the patch length may be detrimental to repair when it exceeds 15.75 (L/t). This limit of patch length give us an economic benefic to reduce the global cost of the repair operation. It has been found that the length (of the recovery) of the repair of the composite leads to a bending response of the repaired pipelines and this length L could be taken as a parameter that could increase the efficiency of the repaired pipes.

d. Development of a predicting model for the repair system

Knowing that the system for repairing pipelines by composite is a function of several parameters, namely the geometry of the crack, the thickness of the pipe, the length of the overlap of the composite, the thickness of the composite. In what follows a nonlinear regression involves all these parameters in a single equation to predict the J integral for a given situation. Nonlinear regression is used to model complex phenomena that do not fall within the linear model. XLSTAT [26], proposes preprogrammed functions among which the user will be able to possibly find the model describing the phenomenon to be modeled.When the desired model is not available, the user has the possibility to define a new model and add it to his personal library.

In this part we summarize a testing and validation analysis of the previously developed model to predict the behavior of the integrated composit-cracked pipe structure. The original model is in the form of a nonlinear multiple regression equation. The model proved to be more accurate in simulating the J integral values of repaired three dimensional through wall cracked pipes (fig.1d) based on our results fig. 7. The general form of the nonlinear model represents a rational framework for developing specific models relevant to the composite overwrap repair technic.

The predicted model :

$$J^{rep} = c_1 + c_2 \mathrm{Exp}\left(c_3 \overline{p}\right) + c_4 \overline{l}^2 + c_5 \overline{a}^2 + c_6 \overline{L} + c_7 \overline{L}^2 \qquad (7)$$

where:

parameters	Value
C_1	-106,8316
C_2	-110,8433
C_3	-1,3366
C_4	0,0011
C_5	864,0942
C_6	9.1156E-3
C_7	3.7582E-4

Table 2: Model's parameters.

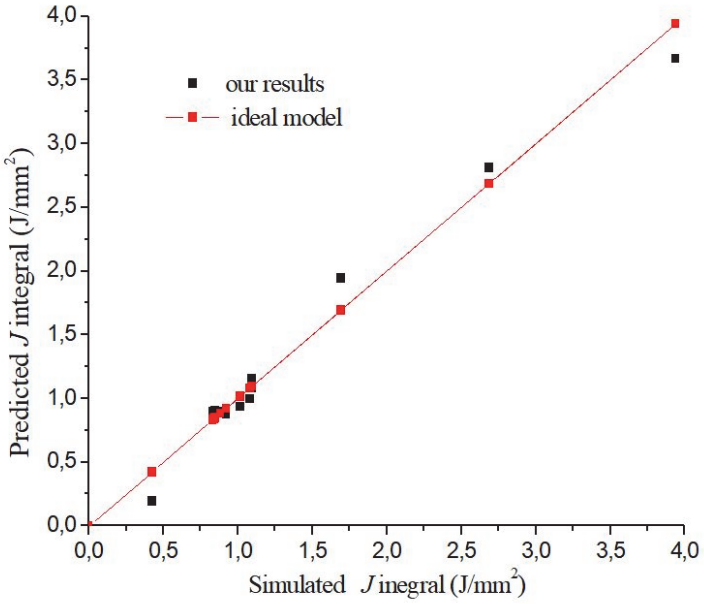

Figure 7: Comparison of the FE results with the predicted model.

The obtained model provides a coefficient of determination R^2= 0,979 with eight degree of freedom and the root of the average squared errors (or residuals) of the model (RMCE) is 0,174 for a convergence criterion about 1E-5.

Second criterion

The aim of pressure vessel design is to avoid structural failure of the vessel during its specified design life.The expression excessive plastic deformation can be used to describe two forms of failure: structural or global failure due to formation of a global plastic collapse mechanism and local failure due to material instability.

In this study, the procedures for limit and elastic-plastic design are considered. Limit analysis assumes an elastic-perfectly plastic material model and small deformation theory. At limit state, any increase of load leads to failure through violation of equilibrium. In design based on limit analysis, the limit load is defined as the load causing gross plastic deformation in the vessel.

To gain confidence in the present FE limit analysis, the plastic limit pressure solutions for uncracked pipes from the present FE analysis are compared with the published solution of Hill [27] and to validate the efficiency of the application of the repaired bonded composite system, by this second criterion we start the validation of our numerical models.

$$\frac{P_L}{\sigma_y} = \frac{2}{\sqrt{3}} ln\left(\frac{R_0}{R_i}\right) \tag{8}$$

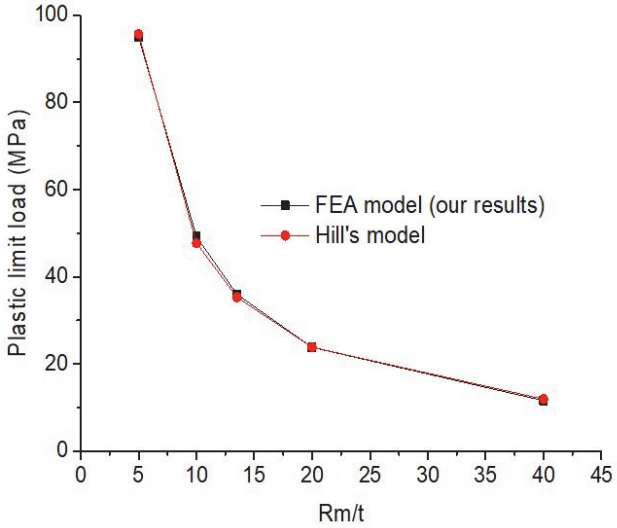

Figure 8: Comparison of the FE limit results for uncracked pipe with HILL's solution.

The results (Fig. 8) show that the present FE analyses agree well with Hill's works. Tabs. 3 validate this observation with maximum error about 3%. Further confidence is gained by comparing for the idealized plane strain case with known solutions for instance Carter's [28] and Chell's [29] works.

Rm/t	FEA model	Hill's model	Error (%)
5,0	95	95,69	0,719
10,0	49,2	47,73	3,086
13,5	36	35,34	1,863
20,0	23,8	23,85	0,207
40,0	11,6	11,92	2,707

Table 2: Relative error between Hill's and our solution

The limit load of pipe with defects under pure internal pressure for Carter and Chell models are given in the Eqns. (9, 10):

Carter's model

$$P_L = \sigma_y \left(\frac{R_0}{R_i + a}\right) ln\left(\frac{R_0}{R_i + a}\right) \tag{9}$$

Chell's model

$$P_L = \frac{2}{\sqrt{3}} \sigma_y \left(\frac{t - a}{R_i + a}\right) \tag{10}$$

The FE limit results for plane strain pipe with extended inner axial crack Fig .1(a) are compared with Chell and Carter's solutions Fig. 9. To avoid mesh problems associated with incompressibility, reduced integration elements within ABAQUS (element type CPE8R) were used in this case. To take into consideration the effect of the crack face, 50% of the internal pressure was applied in this case. In the same scope our results reach agreement with two models and it is more conservative than Chell's model because the consideration of the internal pressure applied on the crack face. For a/t greater than 50% our results converge to Carter's model.

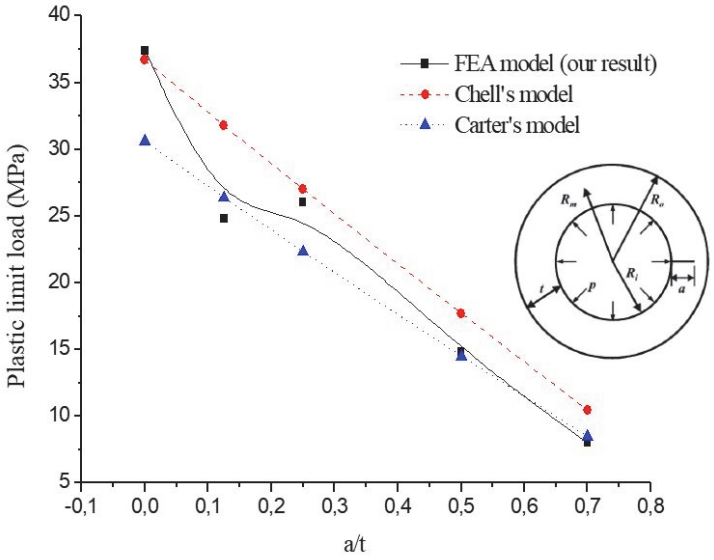

Figure 9: Comparison of the FE limit results for plane strain pipe with extended inner axial crack with Chell's and Carter's solutions.

Carter's and Chell's model are considered a plane strain analysis, another popular work which is Folias's [30] and Erdogan's [31] models investigate three dimensional problems. The dimensions and geometry for axial through-wall cracked pipes (Fig.1d) where Folias's and Erdogan's model was respectively given by Eqn. (11, 12):

$$\frac{P_L R_m}{\sigma_y t} = \frac{1}{\sqrt{1+1.05\sigma^2}} \tag{11}$$

$$\frac{P_L R_m}{\sigma_y t} = \frac{1}{0.614 + 0.87542\sigma + 0.386\exp(-2.275\sigma)} \tag{12}$$

where:

$$\rho = \frac{c}{\sqrt{R_m t}} \tag{13}$$

For the axial through-wall cracked pipes (Fig. 10) compares FEA solution with Folias's and Erdogan's models. this shows that this solution is more conservative than Folias's solution if ϱ<1,5 where it converges to Folia's solution if ϱ>1,5.
Also, this figure validates our FEA model. for this we plot Fig. 11 which will present PLP* (equ. 6) with (c/t) to evaluate the efficiency of the repaired system toward the plastic collapse pressure.
It is visible that the repaired system gives a high beneficial effect on the plastic collapse increasing the plastic limit load up to 220% for a crack length c/t=18. We can complement that in Fig. 11 the PLP* shows an exponential behaviour with crack geometry. To illustrate the efficiency of this repair system, Fig. 12 compares the plastic limit load for cracked pipes for the three models with a repaired pipe.

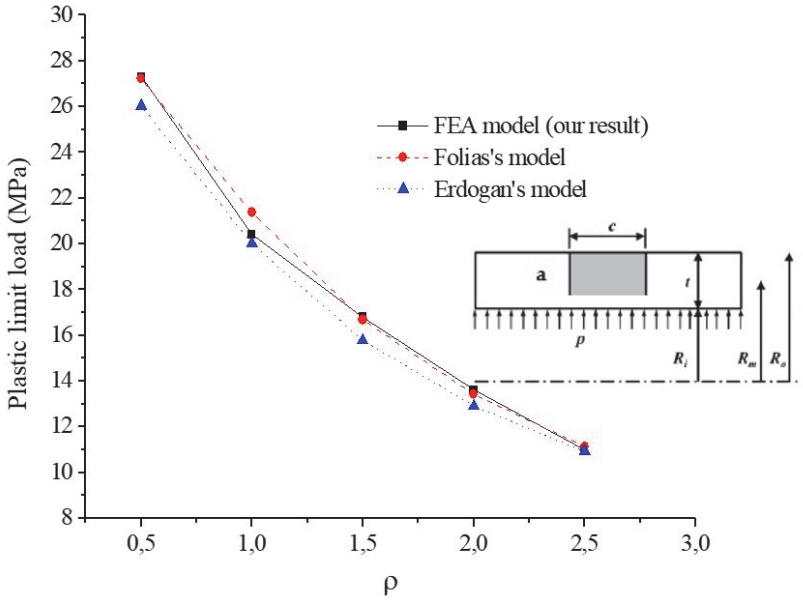

Figure 10: Comparison of the FE limit results with Folias's and Erdogan's solutions for axial through wall cracked pipe.

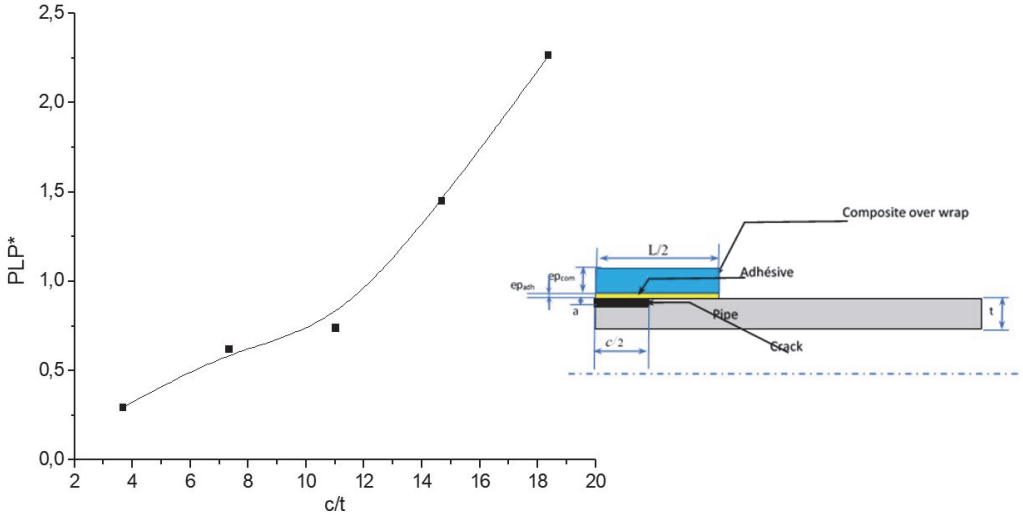

Figure 11: The variation of the PLP* with crack length.

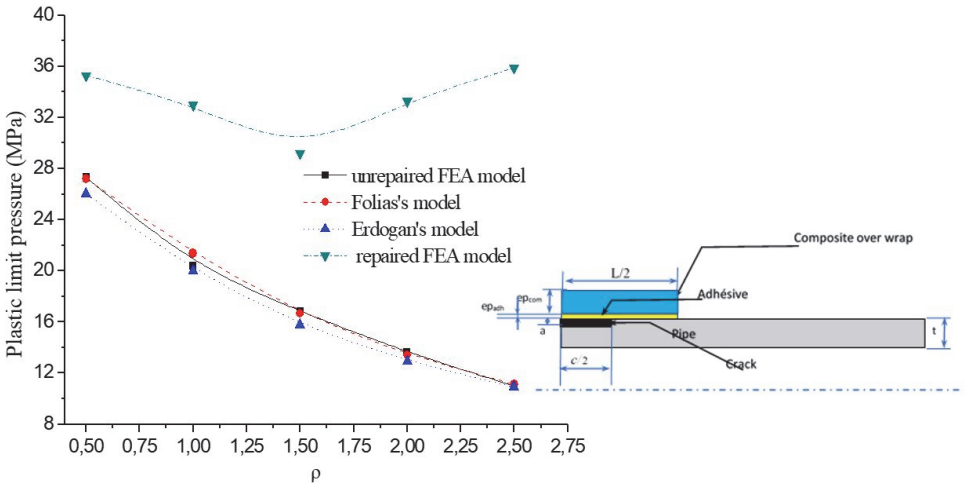

Figure 12: Comparison of the FE limit results with Folias's and Erdogan's solutions.

We note the repaired technic elevate all values of plastic limit load to an average value of PLP = 34 MPa independantly to the crack geometry where, for ϱ=0.5, PLP = 36 MPa and ϱ= 1.5, PLP = 32MPa.
To cover another field where we know that the circumferential crack arises a difficult and dangerous problem regarding non destructive control technic, we evaluate the repair system of through wall circumferential cracked pipes (Fig. 13).

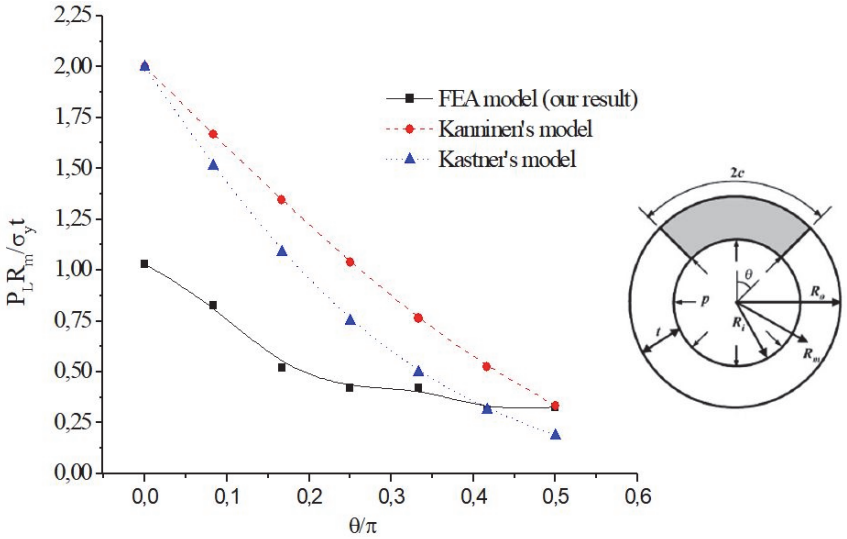

Figure 13: Comparison of the FE limit results for (circumferential through wall - cracked pipe) unrepaired pipe with Kanninen's and Kastner's solution.

Two existing solutions are considered in the present study the most popular limit pressure solution is put forward by Kanninen [32]:

$$\frac{1}{2}\left(\frac{P_L R_m}{\sigma_y t}\right)=1-\frac{\theta+\sin^{-1}\frac{\sin\theta}{2}}{\pi} \tag{14}$$

Another solution is given by Kastner et al [33]:

$$\frac{2}{\left(\frac{P_L R_m}{\sigma_y t}\right)}=\frac{\pi}{\pi-\theta}\left[1+\frac{2\sin\theta\left(\cos\theta+\frac{\sin\theta}{\pi-\theta}\right)}{(\pi-\theta)-\frac{2sin^2\theta}{(\pi-\theta)}-\frac{\sin 2\theta}{2}}\right] \tag{15}$$

In Fig. 13, for larger crack lengths $\frac{\theta}{\pi}$ >0,3 the analytical solutions agree with the FEA results whereas Kastner et al under predict the FEA solutions.
For shorter cracks both analytical solutions over predict the FEA results. The reason for this behavior is that they are based on the assumption that only the axial stress plays a role in plastic collapse thus as $\frac{\theta}{\pi}$ approaches to 0 the limit dimensionless pressure reduces to 2 which is the limit pressure due to axial stress. However, for the uncracked pipes under pressure load, the hoop stress plays a role, not the axial stress, and thus the limit dimensionless pressure approach

to $\frac{2}{\sqrt{3}}$ as validated by Hill's equation (Eqn.. 8) and said before (Fig. 8). The present FEA results shows for $\frac{\theta}{\pi} < 0{,}3$ the hoop stress is dominant in plastic collapse.

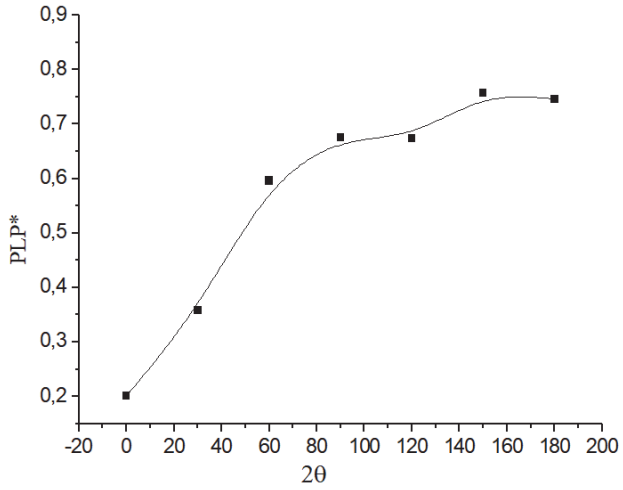

Figure 14: The variation of the PLP* with crack angle for the repaired bonded composite system.

Fig. 14 shows the variation of PLP* with 2θ, it can be seen that the repair system increases the plastic limit load for all circumferential cracks where the PLP* reach a stable level of about 80% for $2\theta > 80°$. In the other hand, we can say that the repair system react three times better in the longitudinal case than the circumferencial cracks. This is due to the level of reaction of the composite overwrap.

CONCLUSIONS

In this work, a numerical limit analysis of API 5L X65 PSL2 steel pressure vessel structure has been studied. Within the scope of this study, the following conclusions can be drawn:

1. A non-linear proportionality behaviour of the value of maximum of J integral with loading.
2. The crack propagation in depth is more dangerous than the longitudinal crack
3. at 150% of the thickness of the pipe the maximum value of the J integral remains constant and independent of the crack length.
4. The composite overwrap reduces the J integral level for a constant value (1.1 J/mm²) beyond 75% of c/t
5. It can be concluded that increasing the patch length may be detrimental to repair when it exceeds 15.75 (L / t). This limit of patch length gives us an economic benefit to reduce the global cost of the repair operation.
6. The results show that the present FE analyses agree well with Hill's works with maximum error about 3%.
7. For a/t greater than 50%, our results converge to Carter's model.
8. For the axial through-wall cracked pipes the FEA solution is more conservative than Folias's solution if $\varrho < 1.5$ where it converges to Folia's solution if $\varrho > 1{,}5$.
9. We note the repaired technic elevate all values of plastic limit load to an average value of PLP = 34 MPa independently to the crack geometry.
10. For through wall circumferential cracked pipes larger crack lengths $\frac{\theta}{\pi} > 0{,}3$ the analytical solutions agree with the FEA results whereas Kastner et al under predict the FEA solutions.
11. The repair system increases the plastic limit load for all circumferential cracks where the PLP* reach a stable level of about 80% for $2\theta > 80°$.

REFERENCES

[1] Walker, R., French, J., Green, M. (2009). Validation testing of composite repair systems for pipes and pipelines, Presentation held at "Pipe Technology. Conference in Hannover.

[2] ASME Boiler & Pressure Vessel Code. (2011). ASME VIII- Rules for construction of pressure vessels division 2, alternative rules. An international code 2011a Addenda.

[3] Inglis, C. E. (1913). Stresses in a plate due to the presence of cracks and sharp corners. SPIE Milestone Series, 137, pp. 3-17.

[4] Irwin, G. (1957) Analysis of Stresses and Strains near the End of a Crack Traversing a Plate. Journal of Applied Mechanics, 24, pp. 361-364.

[5] Irwin, G. R. (1958). Fracture, in Flügge, S. (ed.) Elasticity and Plasticity / Elastizität und Plastizität. Berlin, Heidelberg: Springer Berlin Heidelberg, pp. 551–590. DOI: 10.1007/978-3-642-45887-3_5.

[6] Rice, J. R. (1968). A Path Independent Integral and the Approximate Analysis of Strain Concentration by Notches and Cracks, Journal of Applied Mechanics, 35(2), pp. 379–386. DOI: 10.1115/1.3601206.

[7] Kobayashi, A. S., Chiu, S. T., Beeuwkes, R. (1973). A numerical and experimental investigation on the use of J-integral. Engineering Fracture Mechanics, 5(2), pp. 293–305. DOI: 10.1016/0013-7944(73)90024-6

[8] Hutchinson, J. W. (1968). Singular behaviour at the end of a tensile crack in a hardening material, Journal of the Mechanics and Physics of Solids, 16(1), pp. 13–31. DOI: 10.1016/0022-5096(68)90014-8.

[9] Rice, J. R. and Rosengren, G. F. (1968). Plane strain deformation near a crack tip in a power-law hardening material, Journal of the Mechanics and Physics of Solids, 16(1), pp. 1–12. DOI: 10.1016/0022-5096(68)90013-6.

[10] McClintock, F. A. (1971). Plasticity aspects of fracture, in Engineering Fundamentals and Environmental Effects. Elsevier, pp. 47–225. DOI: 10.1016/B978-0-12-449703-0.50007-2.

[11] Koopman, D. C. A. and Lance, R. H. (1965) 'On linear programming and plastic limit analysis', Journal of the Mechanics and Physics of Solids, 13(2), pp. 77–87. DOI: 10.1016/0022-5096(65)90022-0.

[12] R.H. Lance and D.C.A. Koopman, (1967). Limit analysis of shells of revolution by linear programming, Proc. Tenth Midwestern Mechanics Conf., pp. 225-238.

[13] Berak, E. G. and Gerdeen, J. C. (1990). A Finite Element Technique for Limit Analysis of Structures, Journal of Pressure Vessel Technology, 112(2), pp. 138–144. DOI: 10.1115/1.2928599.

[14] Liu, Y. H., Cen, Z. Z. and Xu, B. Y. (1995). A numerical method for plastic limit analysis of 3-D structures, International Journal of Solids and Structures, 32(12), pp. 1645–1658. DOI: 10.1016/0020-7683(94)00230-T.

[15] Liu, Y., Zhang, X. and Cen, Z. (2004). Numerical determination of limit loads for three-dimensional structures using boundary element method', European Journal of Mechanics - A/Solids, 23(1), pp. 127–138. DOI: 10.1016/j.euromechsol.2003.09.008.

[16] Kim, Yun-Jae et al. (2002). Plastic limit pressures for cracked pipes using finite element limit analyses, International Journal of Pressure Vessels and Piping, 79(5), pp. 321–330. DOI: 10.1016/S0308-0161(02)00031-5.

[17] Liu, P. et al. (2008). Calculations of plastic collapse load of pressure vessel using FEA' Journal of Zhejiang University-SCIENCE A, 9(7), pp. 900–906. DOI: 10.1631/jzus.A0820023.

[18] Miao, X.-T., Zhou, C.-Y. and He, X.-H. (2015). Analysis of Limit Loads for CT Specimens with Cracks Based on Extended Finite Element Method, Procedia Engineering, 130, pp. 763–774. DOI: 10.1016/j.proeng.2015.12.192.

[19] API 5L. Specification for line pipe. APL specification 5L, 42nd ed. USA: TheAmerican Petroleum Institute; 2000.

[20] W. Ramberg, W. R. Osgood (1943). Description of Stress-Strain curves by three parameters.', Washington DC: National Advisory Committee for Aeronautics, Technical Note No.902.

[21] Walker, A. C. and Williams, K. A. (1995) Proceedings of the 14th International Conference on Offshore Mechanics and Arctic Engineering, OMAE 1995: Copenhagen, Denmark, June 18 - 22, 1995. Vol. 5: Pipeline technology. ASME. Edited by American Society of Mechanical Engineers, pp. 345–350.

[22] Hyer, M. W. (2009). Stress analysis of fiber-reinforced composite materials. Updated edition. Lancaster, Pennsylvania: DEStech Publications, Inc.

[23] Belhadri, D. E. et al. (2019). Stress intensity factors analyses for external semi-elliptical crack for repaired gas-pipeline by composite overwrap under pressure, Frattura ed Integrità Strutturale, 13(49), pp. 599–613. DOI: 10.3221/IGF-ESIS.49.55.

[24] Oudad, W. et al. (2017) 'Analysis of the plastic zone under mixed mode fracture in bonded composite repair of aircraft structures', Aerospace Science and Technology, 69, pp. 404–411. DOI: 10.1016/j.ast.2017.07.001.

[25] Shouman, A. and Taheri, F. (2011) 'Compressive strain limits of composite repaired pipelines under combined loading states', Composite Structures, 93(6), pp. 1538–1548. DOI: 10.1016/j.compstruct.2010.12.001.

[26] www.xlstat.com
[27] Hill, R. (1998) The mathematical theory of plasticity. Oxford : New York: Clarendon Press ; Oxford University Press (Oxford engineering science series, 11).
[28] Carter, A.J. (1992). A library of limit loads for FRACTURE-TWO. Nuclear Electric Report TD/SID/REP/0191.
[29] Chell, G.G. (1979). Elastic-plastic fracture mechanics. Applied Science Publishers, pp. 67-105.
[30] Folias, E.S. (1975). On the fracture of nuclear reactor tubes. SMIRT III London, Paper C4/5.
[31] Erdogan, F. (1976). Ductile fracture theories for pressurised pipes and containers, International Journal of Pressure Vessels and Piping, 4(4), pp. 253–283. DOI: 10.1016/0308-0161(76)90001-6.
[32] Zahoor, A., Wilkowski, G.M., Abou-Sayed, I., Marschall, C.W., Broek, D., Sampath, S.G., Rhee, H., & Ahmad, J.I. (1982). Instability predictions for circumferentially cracked Type-304 stainless-steel pipes under dynamic loading. Final report. [BWR].
[33] Kastner, W. et al. (1981). Critical crack sizes in ductile piping, International Journal of Pressure Vessels and Piping, 9(3), pp. 197–219. DOI: 10.1016/0308-0161(81)90002-8.

NOMENCLATURE

a	Crack depth
c	Crack length
L	Composite overwrap length
R_o	The outer diameter
R_m	The medium diameter
R_i	The internal diameter
L_p	Pipe length
t	Pipe thickness
J	J integral
W	Strain energy density
T_i	The components of the traction vector
u_i	The displacement vector components
x, y	The rectangular coordinates
LEFM	Linear Elastic Fracture Mechanics
EPFM	Elastic Plastic Fracture Mechanics
HRR	Hutchinson, Rice and Rosengren equations
FEA	Finite Element Analyses
σ_0	Reference stress
σ_Y	Yield stress
N	Strain hardening component
r, θ	The polar coordinates
P	Pressure loading
PLP	Plastic Limit Pressure
θ	Crack angle
$\overline{P}$	Dimensionless pressure ($\overline{p} = \frac{p}{\sigma_Y}$)
$\overline{l}$	Dimensionless crack length ($\overline{l} = \frac{l}{t}$)
$\overline{L}$	Dimensionless composite overwrap length ($\overline{L} = \frac{L}{t}$)
$\overline{a}$	Dimensionless crack depth ($\overline{a} = \frac{a}{t}$)